FOREX Publication
Open Access | Rapid and quality publishing

International Journal of
Electrical and Electronics Research (IJEER)
Research Article | Volume 12, Issue 2 | Pages 329-337 | e-ISSN: 2347-470X

Improved Power Sharing Strategy for Parallel Connected Inverters in Standalone Micro-grid

Sravanthy Gaddameedhi[1*] and N. Susheela[2]

[1]*Department of Electrical and Electronics Engineering, Sreenidhi Institute of Science and Technology, Telangana, India; sravanthi314@gmail.com*
[2]*Department Electrical and Electronics Engineering, Osmania University, Telangana, India; nsusheela2007@yahoo.com*

***Correspondence:** Sravanthy Gaddameedhi; sravanthi314@gmail.com

ABSTRACT- The primary goal of integrating alternative energy systems such as solar and wind turbines into the power grid using power electronic devices is to meet the growing energy demands. Connecting inverters in parallel effectively enhance power capacity, reliability, and overall system efficiency. However, an uneven power distribution among the inverters is a significant limitation in these parallel connected inverters (PCI). This study focuses on a distributed generation (DG) unit comprising a solar photovoltaic system (SPV) and a battery energy storage system (BESS) connected to voltage source inverters (VSI) 1 and 2. The proposed approach aims to achieve uniform load/power distribution among the inverters with power management, maintaining a constant DC link voltage despite variations in solar irradiation and temperature. Additionally, the strategy targets the reduction of total harmonic distortion (THD) in the load current. The conventional droop control method is restricted in its ability to achieve accurate and uniform power distribution during load changes. An enhanced P-f and Q-E-based droop control technique (EDCT) and a fuzzy logic controller (FLC) has been proposed to address these challenges. Performance analysis using MATLAB/Simulink was conducted with two test cases, and a comparative assessment was carried out with a conventional controller, such as a Proportional Integral Controller (PIC) and Sliding Mode Controller (SMC), to showcase the effectiveness of the developed control technique. The proposed control method ensures equal sharing of active power of 2.5 and 4kW, 2.5 and 7.5kW and reactive powers of 2.5 and 4Vars, 2.5 and 7.5Vars among the inverters for the two cases even during the load change at t=0.5seconds. The settling time for DC link voltage and THD is effectively diminished to 0.03 and 0.25 seconds and 1.18% and 2.87% for the two test case studies of the proposed method, which are much lower than those of existing methods available in the literature.

Keywords: Parallel inverter, Power sharing, SPV, BESS, FLC, SMC, THD

ARTICLE INFORMATION

Author(s): Sravanthy Gaddameedhi and N. Susheela;
Received: 14/01/2024; **Accepted**: 13/03/2024; **Published**: 03/04/2024;
e-ISSN: 2347-470X;
Paper Id: IJEER 1401-12;
Citation: 10.37391/IJEER.120201
Webpage-link:
https://ijeer.forexjournal.co.in/archive/volume-12/ijeer-120201.html

1. INTRODUCTION

Integrating alternative energy sources and microgrids ensures a consistent power supply connected to the distribution network through inverters. Utilizing PCI technology with these sources brings advantages like increased power handling, reduced conversion stress, enhanced efficiency, and diverse applications for controlling motor drive speed. Nonetheless, a crucial concern associated with PCI lies in the uneven power distribution among inverters due to variations in parameters, communication delays, discrepancies in controller designs, differences in inverter capacities, non-identical loads, and variations in line impedance, among other factors. This, in turn, leads to imperfections in current waveforms, generation of Circulating currents, common-mode voltage, and an overall reduction in system efficiency.

The suggested control mechanism is dependable and capable of addressing unforeseen issues like inverter failures, abrupt shutdowns, and communication interruptions or delays. It guarantees precise power distribution, even when communication links with the secondary controller are lost while maintaining effective power-sharing with the primary controllers [1]. This article categorizes and summarizes various power-sharing strategies based on impedance reshaping [2]. A basic and advanced approach for isolated microgrid was suggested to enhance the reactive power distribution of PCI [3]. The CDC technique utilized in inverter-based islanded microgrid systems faces difficulties in delivering satisfactory performance [4]. A novel power management strategy (PMS) is introduced to facilitate power distribution among renewable sources like photovoltaic and wind systems and battery and super capacitor energy storage [5]. Various linear and nonlinear droop control techniques were developed to enhance the performance of PCI in distribution systems. These techniques aim to improve load equal sharing, stability analysis, THD, steady-state, and transient analysis [6]. S-domain admittance-based techniques were introduced to analyze eigenvalues and mode shapes. [7]. A novel hybrid carrier-based PWM technique was developed for parallel-interleaved two-level three-phase VSIs, treated as a unified three-level inverter to mitigate line current ripple [8]. In an islanded microgrid, an FFNN (Feedforward Neural Network) is utilized to achieve equal power sharing among PCI, controlling voltage and frequency

FOREX Publication
Open Access | Rapid and quality publishing
International Journal of Electrical and Electronics Research (IJEER)
Research Article | Volume 12, Issue 2 | Pages 329-337 | e-ISSN: 2347-470X

[9]. A modified droop control technique in a solar-powered microgrid was developed for balanced real and reactive power sharing among inverters [10].

A particle swarm-optimization-based technique was adopted to calculate optimal droop parameters and decrease line impedance for uniform power sharing [11]. A robust technique for implementing virtual impedance is introduced to effectively mitigate voltage distortion issues arising from harmonic loads, surpassing the impact of physical impedances [12]. An arrangement of hierarchical control is formulated for the interconnected VSI system, which improves the utilization of the droop technique [13]. A novel algorithm derived from soccer league dynamics has been employed to fine-tune an optimal hybrid controller for a UPQC linked with solar power and battery storage systems to enhance the power quality, reduce THD and maintain voltage across DC link capacitor [14]. An innovative self-tuning filter, incorporating a unit vector generation scheme, has been created to achieve phase synchronization in both series and shunt filters [15]. This article exhibits the decentralised droop control methodologies within an AC microgrid context, which consists of interconnected DGs, storage units, and loads that function with synchronized control [16]. The preservation of micro-grid voltage and frequency with different impedances and droop gains in single and multi-bus models has been addressed by incorporating virtual impedance and compensating voltage [17].

The existing literature primarily focuses on the utilization of CDC methodology with PI and SM controllers. The adoption of these approaches poses a potential operational failure risk in the proposed configuration, particularly when dealing with abrupt load changes in power-sharing scenarios. Furthermore, the tuning of conventional PI and SM controllers is challenging due to their non-knowledge-based nature. Moreover, the settling time required to reach a constant value is lengthier compared to controllers grounded in artificial intelligence.

2 PROPOSED CONFIGURATION

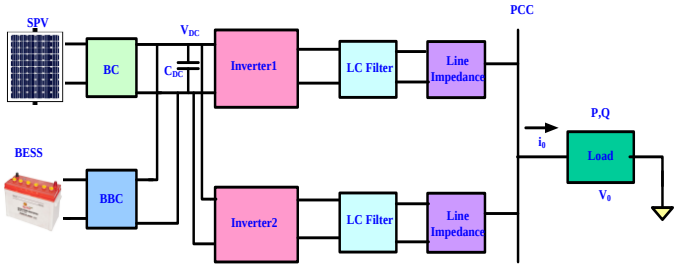

Figure 1. Block diagram of the proposed configuration

The suggested SBS-PCI configuration comprises two VSIs connected in parallel, sharing a common load integrated into a microgrid, which combines SPV and BESS, as given in *figure 1*. The parallel connection of SPV with a DC-to-DC boost converter (BC) and BESS with a DC-to-DC buck-boost converter (BBC) is connected across the inverter input terminals. Additionally, the battery is designed to maintain power management. Various loads are chosen for testing the performance of this configuration. The SPV and BESS enhance the PCI's DC link via BC and BBC, ensuring constant voltage under varying loads and solar irradiation, aiming to minimize converter ratings. *Table I*. outlines the PVS and BESS ratings considered in this study.

2.1 Design of Proposed Configuration

2.1.1 DC Link Voltage

The voltage required across DC link capacitor (V_{DC}) is computed using *eq. (1).*

$$V_{DC\min} = \frac{2\sqrt{2}(V_L)}{\sqrt{3}(m)} \quad (1)$$

Where V_L is the RMS line voltage, and m is the modulation index.

2.1.2 DC Link Capacitor and Boost Inductor

Eq. (2) allows for determining the minimum amount of DC link capacitance and inductance of the boost converter required.

$$C_{DC\min} = \frac{(\frac{P_{PV}}{V_{DC}})}{4\pi f \Delta V_{DC}} \quad \text{and} \quad L_{SPV} = \frac{V_{mpp} D}{\Delta I_{mpp} * f_{sw}} \quad (2)$$

Where fsw is the switching frequency, ΔImpp is chosen as the 20% of PV current under maximum power point

2.1.3 LC Filter

The modeling equations of filter inductances and capacitance are given below in *eq. (3-4).*

$$L_f = \frac{\sqrt{3} m V_{DC}\ \omega_{sw}}{12(2\pi)\Delta i_{\max}} \quad (3)$$

$$C_f = x * C_b \quad (4)$$

$$C_b = \frac{P}{\omega_f V_L^2}, \quad 10\omega_f < \omega_{res} < \frac{1}{2}\omega_{sw}$$

Where ω_{sw} is the inverter angular switching frequency, ΔImax is the maximum current ripple (10% to 25% of nominal phase current), x is the filter capacitance factor that should be less than 15% of base capacitance Cb, and ωf is the filter frequency.

2.2 External Support for DC Link

The SPV and BESS contribute to enhancing the stability of the PCI in addressing power-sharing issues by supporting the DC-bus through a BC, and B-B-C. The power at the PCC is expressed by *eq. (5).*

$$P_{SPV} + P_{BESS} - P_{DClink} = 0 \quad (5)$$

2.2.1 SPV Modelling

Solar energy is a non-conventional and highly favored energy source compared to conventional resources due to its abundant and clean nature, posing no harm to the environment. The inverters can be smoothly integrated with solar energy. PV

FOREX Publication
Open Access | Rapid and quality publishing
International Journal of Electrical and Electronics Research (IJEER)
Research Article | Volume 12, Issue 2 | Pages 329-337 | e-ISSN: 2347-470X

panels are set up in a series/parallel arrangement to yield the needed power. DC-DC boost converters help raise the solar panels' power to the required level. These panels charge the DC link capacitor and exchange real power to match supply and demand. Therefore, getting the most power from the solar panels is crucial, achieved through the MPPT controller. The Incremental Conductance algorithm is considered to get the maximum power from the SPV. *Figure 2* shows the PV system controller and the basic PV cell model, and *eq. (6)* calculates the PV panel's maximum output power.

$$P_{SPV\max} = V_{SPV\max} * i_{SPV\max} \quad (6)$$

Where, $V_{PV\max}$, and $I_{PV\max}$ are the values of maximum output voltage and current PV panel.

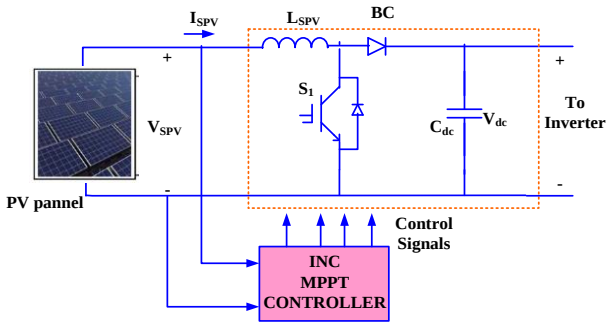

Figure 2. SPV with BC

2.2.2 Battery Modeling

The BESS is comprised of a battery and a BBC, accountable for regulating the V_{dc}, as depicted in *figure 3*. The state of charge (SoC) is determined by *eq. (7).*

$$SoC = 80(1 + \int i_{BESS} dtQ) \quad (7)$$

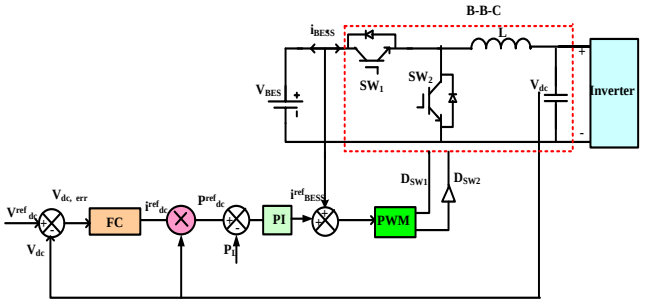

Figure 3. BESS with BBC

The battery operates in dual phases: charging and discharging, depending on solar power generation. Its functionality is dictated by energy constraints, specifically the SoC limits outlined in *eq. (8).*

$$SoC_{\min} \le SoC \le SoC_{\max} \quad (8)$$

Where Q is the battery capacity, and i_{BESS} represents the current flowing through the battery.

The reference current i^{ref}_{dc} is estimated by minimizing the DC link voltage error $V_{dc,\,error}$ through a FC. In mathematical terms, this approximation is detailed in *eq. (9).* The battery current is added to the, i^{ref}_{BESS}, and the required PWM pulses are generated to activate the switches in the buck-boost converter. This process can be expressed mathematically as outlined in *eq. (10-12)*, where k_p and k_i represent two constant values denoting the PI controller's proportional gain and integral gain. These values are set to 0.9 and 65, respectively.

$$V_{dc,error} = V^{ref}{}_{dc} - V_{dc} \quad (9)$$

$$P^{ref}{}_{dc} = i^{ref}{}_{dc} V_{dc} \quad (10)$$

$$P_{err} = P^{ref}{}_{dc} - P_L \quad (11)$$

$$i^{ref}_{BES} = K_p P_{err} + K_i \int_0^t P_{err} dt \quad (12)$$

Table I. SPV and Bess Specifications

Device	Parameters	Values
PV panel (Sun Power SPR-215-WHT-U)	Output power	305.226 W
	Open circuit voltage	64.2 V
	Short circuit current	5.96 A
	Under max power, V& I	54.7 V/5.58 A
	Number of PV cells assembled in series and parallel	12 & 3
	R_{SPV}, L_{SPV} and C_{SPV}	0.005 Ω, 5 mH and 100 µF
BESS	Rated capacity	12 Ah
	Maximum Capacity	6000 Ah
	Rated Voltage	500 V
	Full Charge Voltage	544.4 V
	L_{BESS} and C_{BESS}	0.35 mH and 250 µF

3. METHODOLOGY

3.1 Droop Control Technique (DCT)

The DCT technique regulates a distribution system's active and reactive powers [10]. Typically, the angular frequency and voltage provided by *eq. (13 & 14)* control the active and reactive powers.

$$\omega = \omega^* - m(P_{cal} - P^*) \quad (13)$$

FOREX Publication
Open Access | Rapid and quality publishing
International Journal of Electrical and Electronics Research (IJEER)
Research Article | Volume 12, Issue 2 | Pages 329-337 | e-ISSN: 2347-470X

$$E = E^* - n(E_{cal} - E^*) \quad (14)$$

Where m and n are the inverter droop coefficients for frequency and voltage, respectively; P* and Q* are the nominal real and reactive powers; the rated voltage is denoted by E*, and the nominal angular frequency is ω*. *Figure 4* displays the block diagram of DCT and *figure 5* shows the graphical representation of droop characteristics respectively.

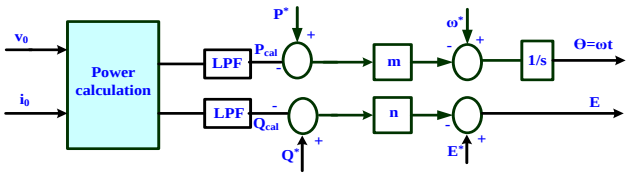

Figure 4. Block diagram of DCT

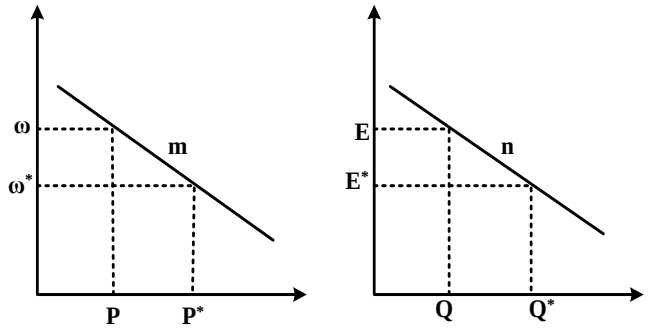

Figure 5. Droop characteristics

3.1.1 Selection of droop coefficients

Where, $\Delta\omega_{max}$ and ΔV_{max} are decided based on the maximum deviations allowed in the load. The droop coefficients will affect the power sharing among inverters, where larger droop coefficients lead to better power sharing. However, increasing them would lead to instability in the system. This conventional droop control method fails to achieve precise sharing of real and reactive power when there are fluctuations in frequency and voltage due to load changes in the micro grid. An enhanced droop control method is suggested to address this issue.

$$m = \frac{\Delta\omega_{max}}{P_{max} - P_{min}} \quad (15)$$

$$n = \frac{\Delta V_{max}}{Q_{max} - Q_{min}} \quad (16)$$

3.2 Enhanced Droop Control Technique (EDCT)

To maintain a steady operating frequency that remains unaffected by variations in load and ensures precise active power, the Frequency Restoration Scheme (FRS) has been introduced. *Figure 6* illustrates this situation for two inverters arranged in a back-to-back configuration, with the droop curves connected. Here, points 'a' and 'a" represent the state before the load variation, maintaining the rated operating frequency ω*. As the load changes from P_1 to P_1', the operating points shift from 'b' to 'b", indicating a reduced operating frequency. To ensure a consistent frequency and accurate active power, it is crucial to uniformly elevate the droop characteristics between the inverters until they intersect at points 'c' and 'c". This process is called the FRS and it is used to bring the frequency back to its specified nominal value, ω*, by integrating the δω term into *eq. (13)* for adjustment.

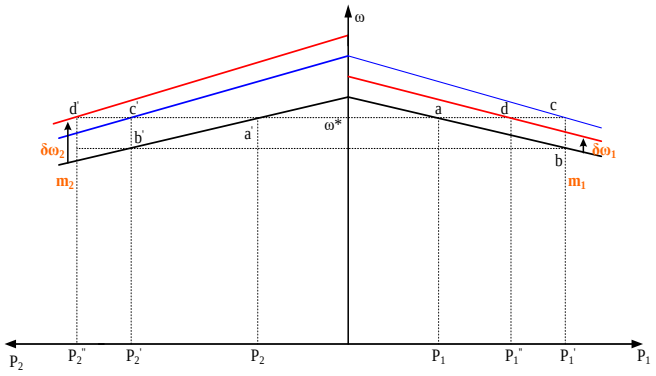

Figure. 6 Droop curves adjustments for real power sharing among the inverters

$$\omega = \omega^* + \delta\omega - m(P^* - P_{cal}) \quad (17)$$

From *eq. (17),* For acquiring ω = ω*, the δω must be equal to $m(P^*-P_{cal})$. Thus, δω is modified so that in the steady state, $\delta\omega = m(P^*-P_{cal})$. To achieve this, δω is reformed as:

$$\frac{d}{dt}(\delta\omega) = K\Delta\omega \quad (18)$$

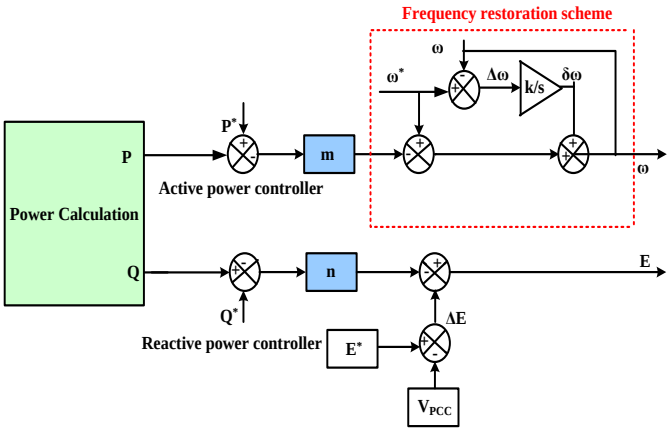

Figure 7. Block diagram for EDCT

FOREX Publication
Open Access | Rapid and quality publishing
International Journal of Electrical and Electronics Research (IJEER)
Research Article | Volume 12, Issue 2 | Pages 329-337 | e-ISSN: 2347-470X

Accurate frequency restoration without errors necessitates the uniform distribution of δω among all VSIs. To achieve this, the FRS must be simultaneously integrated into two inverters. The vertical displacement value of each VSI, denoted as δω, is determined by the integral of Δω, as illustrated in figure 7. Reactive power distribution among the inverters is achieved via DCT, as it is not changing. However, variations arise when there is a difference in line impedances of two inverters or the addition of local loads. In the proposed configuration, the impedances of the two inverters are assumed to be equal, and no local loads are present. Consequently, reactive power sharing is exclusively conducted through the DCT method.

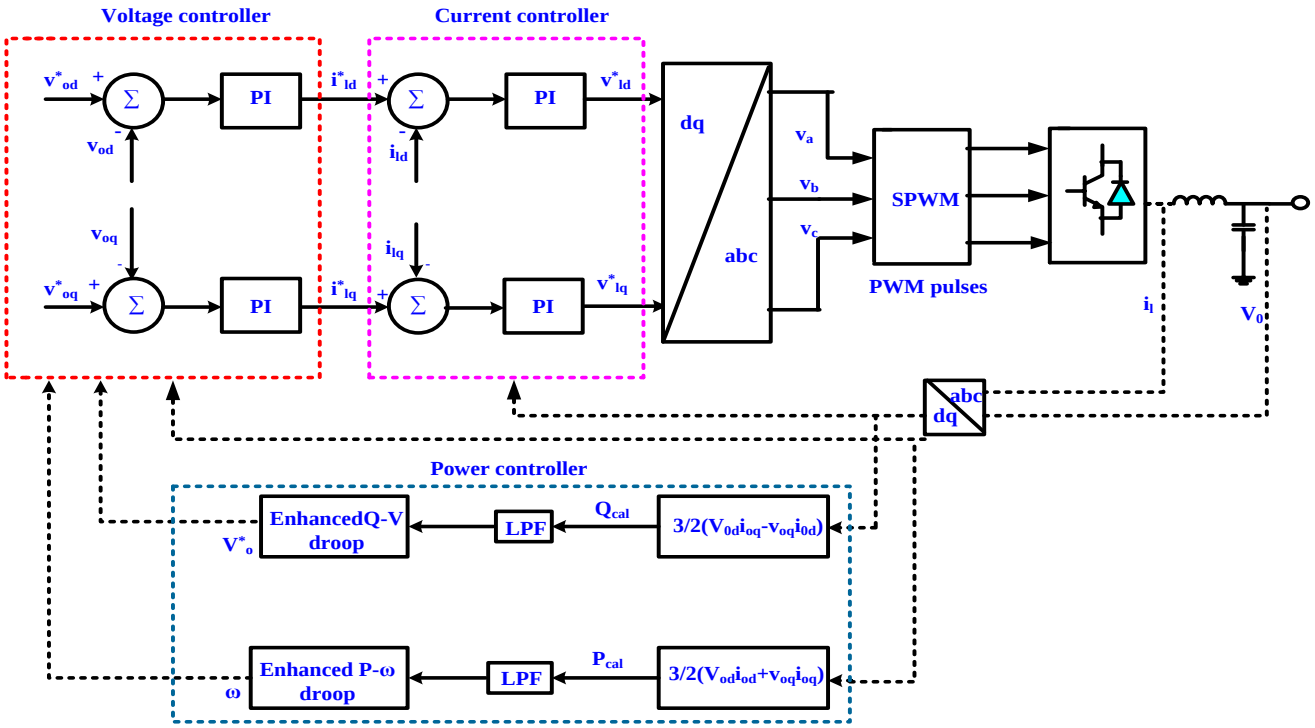

Figure 8. Voltage and current controllers

The control of VSI involves three loop controls: an outer loop for power control, a middle loop for controlling the voltage, and an inner loop to regulate the current. Where reference output voltage signal of the external power loop is given to the voltage control loop and this loop produces the reference current signals. These current signals will give to the inner current control loop. This current loop compares the actual signal with a reference signal and generates appropriate firing pulses to the inverter switches. The control diagram of the proposed control technique is shown in *figure 8*. The proposed system ratings are given in *table II*. The real and reactive power corresponding to the fundamental components is extracted with the help of a low pass filter, and it is given by,

$$P_1 = \frac{\omega_C}{s+\omega_C} P_{cal} \quad \text{and} \quad Q_1 = \frac{\omega_C}{s+\omega_C} Q_{cal} \qquad (19)$$

Here, ωc is filter gain, K_{pv},K_{iv} are the PI controller gains, V_{od}, V_{oq}, i_{od} and i_{oq} are the inverter1 dq0 frame voltages and currents V^*_{od}, V^*_{oq} are the reference output voltage of inverter in dq frame, V_{ld}, V_{lq} are the output voltage of inverter in dq frame before filter, V^*_{ld}, V^*_{lq} are the reference output voltage of inverter in dq frame before filter, i^*_{od}, i^*_{oq} are the inverter reference output current in dq frame, i_{ld}, i_{lq} are inverter output current before filter, and i^*_{ld}, i^*_{lq} are the inverter reference output currents before the filter.

Table II. Ratings of the Developed System

Parameter	Value
DC supply	700V
Rated AC voltage and frequency	380 V, 50 Hz
Carrier frequency	10 kHz
P_F, Q_E Co-efficient	m= 1e-5, and n = 2e-4
R_f. L_f and C_f	0.01Ω , 2.5mH, and 10μF
Inner current loop and Outer voltage loop	K_p=0.01, and K_i=50 and K_p=0.05, and K_i=100
DC link capacitor and voltage	350μF & 700 V
Load	Case 1: P=8 kW, Q=800 VARs Case 2: P=15 kW, Q=1500 VARs (P_1=5kW, t=0 to 0.5sec and P_2=15kW, t=0.5 to 1sec)

3.3 Fuzzy Controller

The functioning of the FLC serves as an intelligent controller that depends on linguistic rules for decision-making. Its fundamental elements comprise an inference engine, rule base, fuzzifier, defuzzifier, and knowledge base. The function of the fuzzifier involves translating numerical inputs into linguistic variables by employing membership functions (Msf). The knowledge base retains current data regarding input-output

FOREX Publication
Open Access | Rapid and quality publishing
International Journal of Electrical and Electronics Research (IJEER)
Research Article | Volume 12, Issue 2 | Pages 329-337 | e-ISSN: 2347-470X

correlations. The inference engine employs the rule base and Msf to ascertain suitable actions. Ultimately, the defuzzifier converts fuzzy variables into precise outputs. The outline of the FLCs process is illustrated in *figure 9*.

$$E = V^{ref}{}_{dc} - V^{k}{}_{dc};\ k = 1,2,3,4,5,6 \qquad (20)$$

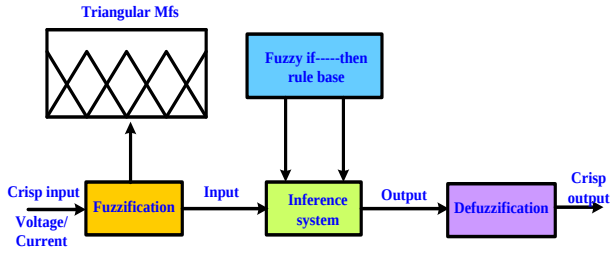

Figure 9. Outline of FLC

Fuzzification is the first layer, and its outputs are fuzzy MSF, which are determined by *eq. (21).*

$$\mu_{Ai}(x), i = 1,2.$$
$$\mu_{Bj}(y), j = 1,2. \qquad (21)$$

Here, μ_{Ai} μ_{Bj} resembles the memberships received as the output from the 1st layer.

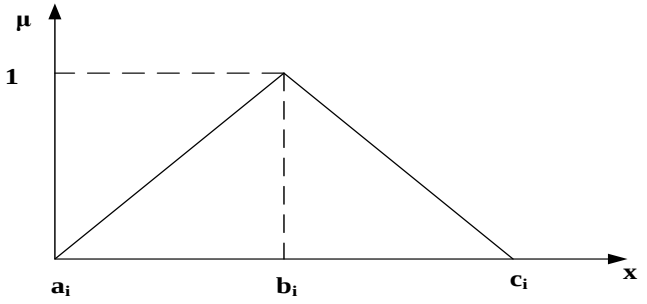

Figure 10. Triangular membership

The triangular membership is shown in *figure 10* and it is is expressed by *eq. (22).*

$$\mu_{Ai}(x) = \max(\min(\frac{x - a_i}{b_i - a_i}, \frac{c_i - x}{c_i - b_i}), 0) \qquad (22)$$

Where, b_i is the fuzzy set i's point of greatest support and x_{min}, x_{max} (lower and upper bonds) is the range (world of discourse) of x. Under normalization, -1 and 1 are regarded as lower and upper bonds in this work.The presented study utilizes the Takagi-Sugeno approach, utilizing E *(obtained from eq.20)* and CE as inputs for the system. Triangular membership functions (Msfs) denote fuzzy variables: BPS, MPS, SPS, ZR, BNG, MNG, and SNG. These linguistic terms correspond to the V_{dc} levels and are outlined in *figure 11 to 12*. These terms are structured into 49 sets of Msfs, as comprehensively outlined in Table III.

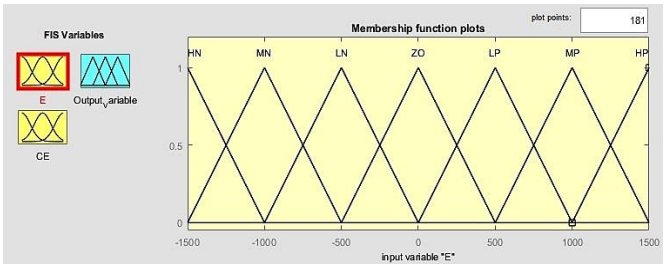

(a)

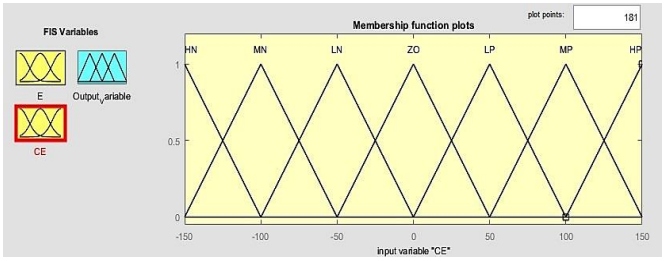

(b)

Figure 11. (a) Msf of E, (b) Msf of CE

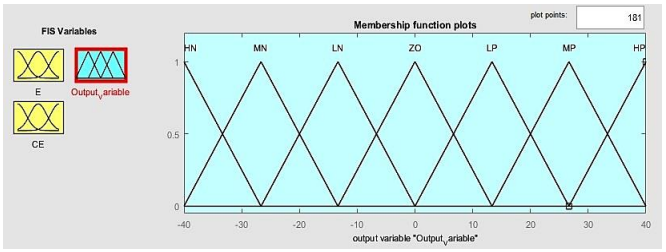

Figure 12. Msf of Output

Table III. MSF for DC Link Voltage

Error	CE						
	BPS	MPS	SPS	ZR	SNG	MNG	BNG
BNG	ZR	SNG	MNG	BNE	BNG	BNG	BNG
MNG	SPS	ZR	SNG	MNG	BNG	BNG	BNG
SNG	MPS	SPS	ZR	SNG	MNG	BNG	BNG
ZR	BPS	MPS	SPS	ZR	SNG	MNG	BNG
SPS	BPS	BPS	MPS	SPS	ZR	SNG	MNG
MPS	BPS	BPS	BPS	MPS	SPS	ZR	SNG
BPS	BPS	BPS	BPS	BPS	MPS	SPS	ZR

4. RESULTS AND DISCUSSION

The proposed SBS-PCI was developed in MATLAB Simulink environment. To analyze the performance of the suggested method, two case studies are considered with two different loads and it is illustrated in *table IV*. The inverter1 and inverter2 output voltage/current, voltage and current at the load terminals and active/reactive power sharing were analyzed. In addition, the THD was obtained for the proposed system, and further, it is compared with the PI controller, as illustrated in *table V*.

FOREX Publication
Open Access | Rapid and quality publishing
International Journal of Electrical and Electronics Research (IJEER)
Research Article | Volume 12, Issue 2 | Pages 329-337 | e-ISSN: 2347-470X

Table IV. Types of Loads

Type of Load	Case-1	Case-2
Load1: Three-phase Linear Load P=5 kW and Q_L=500VARs (t=0 to 0.5sec) P=8 kW and Q_L=800 VARs (t=0.5 sec to 1sec) (Less than PV power)	✓	
Load2: Three-phase Linear Load P=5 kW and Q_L=500VARs (t=0 to 0.5sec) P=15 kW and Q_L=1500 VARs (t=0.5 sec to 1sec) (greater then PV power)		✓

Case 1: In this analysis, Load 1 is taken into consideration to evaluate the proposed technique. The output voltage/current waveforms of Inverter 1 and Inverter 2 are presented in *figure 13(a) and 13(b)*, respectively. The load voltage/current waveforms are displayed in *figure 13(c)*. Additionally, *figure 13(d)* provides total active and reactive powers at the load. Finally, *figure 13(e)* demonstrates that the suggested method achieves equal sharing of real and reactive powers between the inverters. This is accomplished through an enhanced droop control technique with FLC implementation. However, the solar power changes by varying the solar irradiation; accordingly, the battery will charge and discharge to maintain the constant power at load, as shown in *figure 13(f)*. This figure clearly shows that the suggested FLC controller maintains the DCL voltage is constant with low settling time even under transient conditions such as variations in solar irradiation as compared to the PIC and SMC.

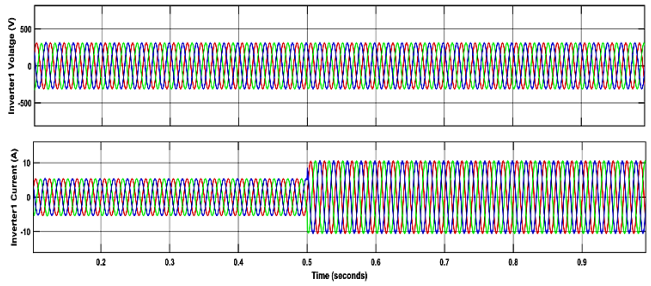

(a)

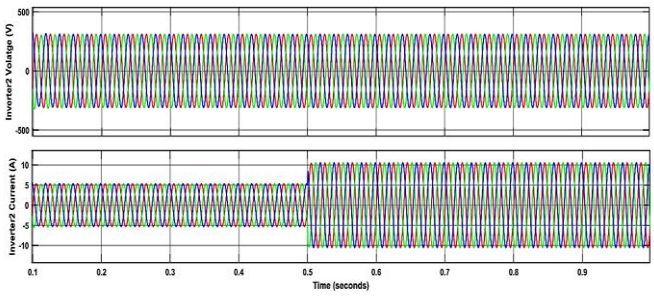

(b)

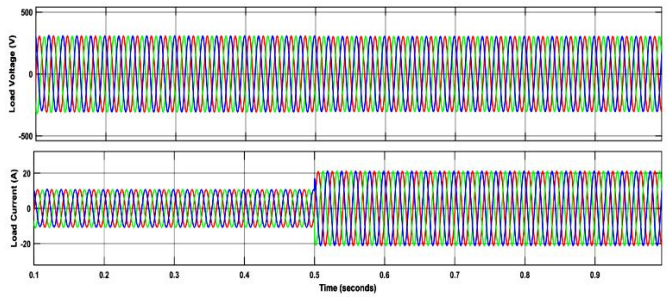

(c)

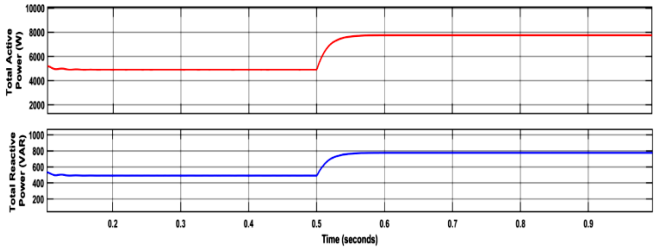

(d)

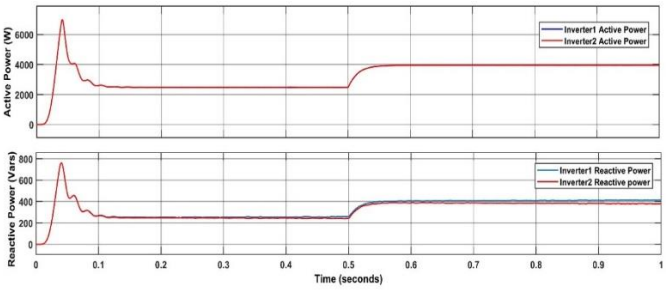

(e)

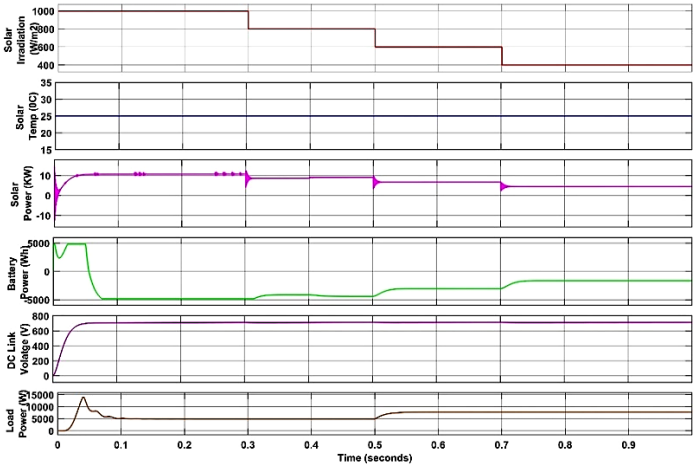

(f)

Figure 13. (a) V/I waveforms of inverter 1 (b) V/I of inverter 2 (c) Voltage and current waveforms at load (d) Total active and reactive power waveforms (e) Active and reactive power sharing waveforms (e) Solar power, battery power with variable irradiation and constant DCL voltage and load power of 8 kW

FOREX Publication
Open Access | Rapid and quality publishing
International Journal of Electrical and Electronics Research (IJEER)
Research Article | Volume 12, Issue 2 | Pages 329-337 | e-ISSN: 2347-470X

Case 2: The superior performance of the developed method is demonstrated by considering the combination of Load 1 and Load 2. *Figure 14(a)* displays the output voltage/current waveforms. This figure shows that the load current increases from 20A to 30A as the load changes from 5kW to 15kW.

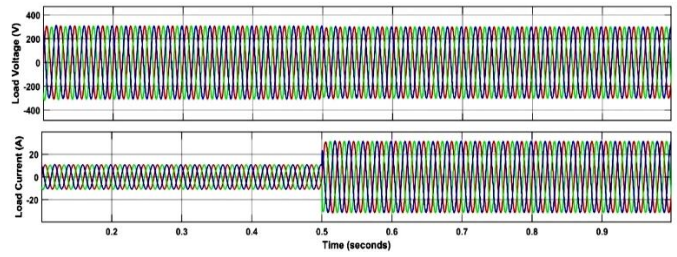

(a)

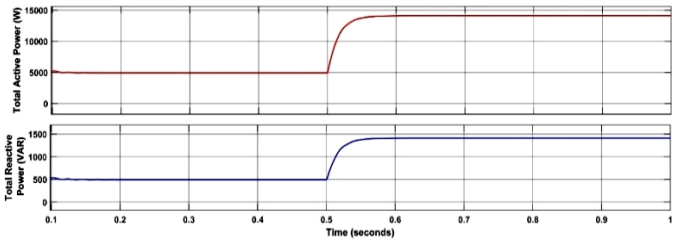

(b)

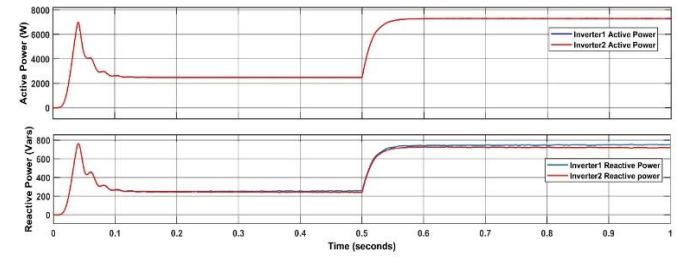

(c)

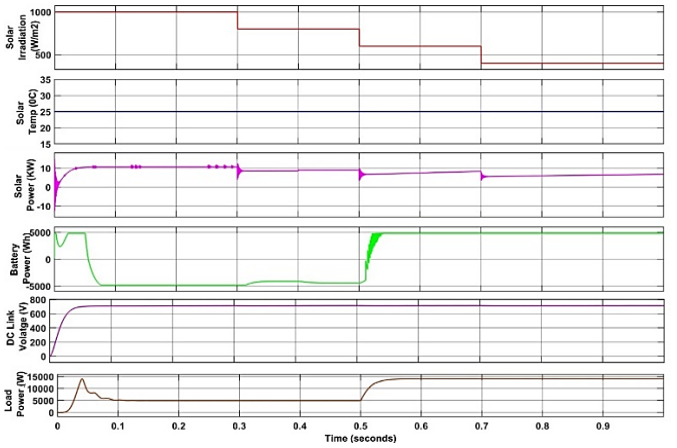

(d)

Figure 14. (a) Load V & I waveforms, (b) Total active and reactive power waveforms (c) Active and Reactive power sharing waveforms (d) Solar power, battery power, voltage at DC link and load power with variable irradiation and constant temperature

Figure 14(b) gives total active and reactive power available at the load. The proposed controller effectively ensures equal control of active and reactive powers among the inverters using the proposed technique, even when there is a load change at t=0.5 sec. This is evident in *figure 14(c).* However, with variable solar irradiation, the solar power undergoes changes, leading to corresponding charging and discharging of the battery to sustain a consistent power supply to the load, as depicted in *figure 14(d).* This figure distinctly illustrates that the suggested FLC effectively maintains a consistent DCL voltage even in the presence of variations in solar irradiation. Furthermore, the proposed system frequency is maintained as constant, as shown in *figure 15*. The harmonic distortion for two cases was obtained and exhibited in *figure 16*.

Table V. %THD Comparison

Controller	Case 1 (%)	Case 2 (%)
PI	4.21	4.79
SMC	3.65	4.01
Proposed FLC	**1.18**	**2.87**

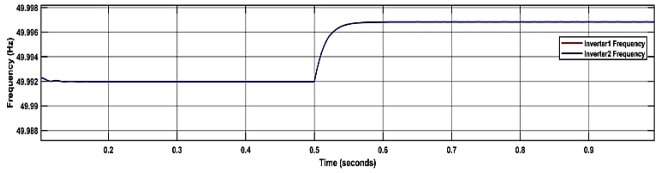

Figure 15. Frequency waveform

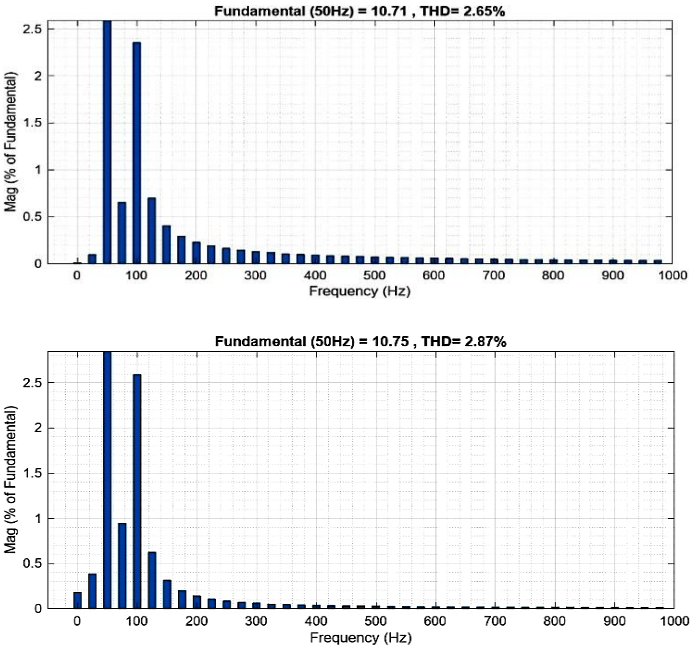

Figure 16. Frequency waveform

5. CONCLUSION

This study focused on the operation and control of a solar battery integrated Parallel Connected Inverter (SBS-PCI). An EDCT technique along with the FLC was proposed to address the uniform distribution of power during load change over the conventional droop control technique, and it was compared with

International Journal of
Electrical and Electronics Research (IJEER)
Research Article | Volume 12, Issue 2 | Pages 329-337 | e-ISSN: 2347-470X

a PI controller. Through simulation in MATLAB, the results demonstrated excellent performance of the proposed approach in achieving the objectives, which include equal power/load sharing among the two inverters, management of power, constant DC link voltage across the capacitor, and reduction in the THD of the load current. The application of proposed technique results in the equal sharing of active power of 2.5 and 4kW, 2.5 and 7.5kW and reactive powers of 2.5 and 4Vars, 2.5 and 7.5Vars among the inverters for the two cases even during the load change at t=0.5seconds. The settling time for DC link voltage and THD is effectively diminished to 0.03 and 0.25 seconds and 1.18% and 2.87% for the two test case studies of the proposed method, which are much lower than those of existing methods available in the literature. As a future study, it is recommended that this work be extended by incorporating a hybrid controller, which can further enhance the performance and efficiency of the system.

Limitations of Research Work

• In the proposed configuration, identical renewable energy source in association with energy storage system was considered for both the inverters instead of different renewable sources.

• In this developed method the unbalanced load was not considered due to large unequal power sharing which cannot be handled by suggested topology.

Scope for Future Work

• The proposed configuration can be implemented with more than two parallel connected inverters.

• It can be modified to perform with Neutral point clamped (NPC) inverters instead of VSI.

Author Contributions: 1. Sravanthy Gaddamedhi- Conceptualization, methodology, and writing—original draft preparation.

2. N. Susheela- Supervision

REFERENCES

[1] N. Mohammed, A. Lashab, M. Ciobotaru and J. M. Guerrero, "Accurate Reactive Power Sharing Strategy for Droop-Based Islanded AC Microgrids," in IEEE Transactions on Industrial Electronics, vol. 70, no. 3, pp. 2696-2707, March 2023, doi: 10.1109/TIE.2022.3167141.

[2] F. Deng, W. Yao, X. Zhang, Y. Tang and P. Mattavelli, "Review of Impedance-Reshaping-Based Power Sharing Strategies in Islanded AC Microgrids," in IEEE Transactions on Smart Grid, vol. 14, pp. 1692-1707, May 2023, doi: 10.1109/TSG.2022.3208752.

[3] A. Smadi and L. I. Shehadeh, "An Improved Reactive Power Sharing in an Isolated Microgrid with a Local Load Detection," in Chinese Journal of Electrical Engineering, vol. 9, no. 2, pp. 14-26, June 2023, doi: 10.23919/CJEE.2023.000021.

[4] Rashwan, A.; Mikhaylov, A.; Senjyu, T.; Eslami, M.; Hemeida, A.M.; Osheba, D.S.M. Modified Droop Control for Microgrid Power-Sharing Stability Improvement. Sustainability 2023, 15, 11220. https://doi.org/10.3390/su151411220.

[5] S. Patel, A. Ghosh, P. K. Ray and V. Gurugubelli, "Effective Power Management Strategy and Control of a Hybrid Microgrid with Hybrid Energy Storage Systems," in IEEE Transactions on Industry Applications, doi: 10.1109/TIA.2023.3303862.

[6] P. Monica, M. Kowsalya, Control strategies of parallel operated inverters in renewable energy application: A review, Renewable and Sustainable Energy Reviews, Volume 65,2016, Pages 885-901, ISSN 1364-0321, https://doi.org/10.1016/j.rser.2016.06.075

[7] Sulaiman Z. Almutairi, "Dynamic Interactions between Parallel Grid-Forming Inverters in a Microgrid", Applied Sciences, vol.13, no.12, pp.6989, 2023.

[8] M. Varun, K. Shukla, R. Maheshwari and A. K. Jain, "A new hybrid PWM for two parallel connected interleaved two-level inverters to reduce output current ripple," 2017 IEEE 7th International Conference on Power and Energy Systems (ICPES), Toronto, ON, Canada, 2017, pp. 74-79, doi: 10.1109/ICPESYS.2017.8215924.

[9] T. Vigneysh & N. Kumarappan (2016) Artificial Neural Network Based Droop-Control Technique for Accurate Power Sharing in an Islanded Microgrid, International Journal of Computational Intelligence Systems, 9:5, 827-838, DOI: 10.1080/18756891.2016.1237183.

[10] N.S. Suresh, S. Arul Daniel, Novel droop-based controller for parallel connected solar inverter in a microgrid, Materials Today: Proceedings, Volume 46, Part 19,2021, Pages 10102-10108, ISSN 2214-7853.

[11] Fatih Cingoz, Ali Elrayyah & Yilmaz Sozer (2015) Optimized Droop Control Parameters for Effective Load Sharing and Voltage Regulation in DC Microgrids, Electric Power Components and Systems, 43:8-10, 879-889, DOI: 10.1080/15325008.2015.1021220.

[12] J. He and Y. W. Li, "Analysis, Design, and Implementation of Virtual Impedance for Power Electronics Interfaced Distributed Generation," in IEEE Transactions on Industry Applications, vol. 47, no. 6, pp. 2525-2538, Nov.-Dec. 2011, doi: 10.1109/TIA.2011.2168592.

[13] W. Yao, M. Chen, J. Matas, J. M. Guerrero and Z. -M. Qian, "Design and Analysis of the Droop Control Method for Parallel Inverters Considering the Impact of the Complex Impedance on the Power Sharing," in IEEE Transactions on Industrial Electronics, vol. 58, no. 2, pp. 576-588, Feb. 2011, doi: 10.1109/TIE.2010.2046001.

[14] Koganti Srilakshmi, Nakka Srinivas, Praveen Kumar Balachandran, Jonnala Ganesh Prasad Reddy, Sravanthy Gaddameedhi, "Design of Soccer League Optimization Based Hybrid Controller for Solar-Battery Integrated UPQC," in IEEE Access, vol. 10, pp. 107116-107136, 2022, doi: 10.1109/ACCESS.2022.3211504.

[15] Koganti Srilakshmi, Sravanthy Gaddameedhi, Uday Kumar Neerati, Surender Reddy Salkuti, Ponamanenni Anoop Rao, Thattiparthi Pavan Kumar, Performance Analysis of Fuzzy-Based Controller for Wind and Battery Fed UPQC, Power Quality in Microgrids: Issues, Challenges and Mitigation Techniques. Lecture Notes in Electrical Engineering, vol 1039. Springer, Singapore. https://doi.org/10.1007/978-981-99-2066-2_11.

[16] S. G. Ndeh, B. J. Ebot, A. F. Akawung, N. D. Khan and T. Emmanuel, "Decentralized Droop Control Strategies for Parallel-Connected Distributed Generators in an AC Islanded Microgrid: A Review," 2023 7th International Conference on Green Energy and Applications (ICGEA), Singapore, Singapore, 2023, pp. 83-90, doi: 10.1109/ICGEA57077.2023.10126012.

[17] A. Ketabi, S. Rajamand, M. Shahidehpour, "Power Sharing in Parallel Inverters with Different Types of Loads", IET Generation, Transmission & Distribution, vol. 11, no. 10, p. 2438-2447, 2017. https://doi.org/10.1049/iet-gtd.2016.0570.